Parametric Study of a Stationary Plasma Thruster using a Two-Dimensional Hybrid Model[*♠]

G.J.M. Hagelaar, J. Bareilles, L. Garrigues, and J.P. Boeuf
CPAT, Bâtiment 3R2
Université Paul Sabatier
118 Route de Narbonne
31062 Toulouse
France
hagelaar@cpat.ups-tlse.fr

IEPC-01-28

A 2D model of a stationary plasma thruster has been developed. The model is based on a collisionless treatment of ions and neutral atoms, coupled with a fluid description of electron transport assuming quasi-neutrality. The results reproduce the low frequency oscillations due to neutral depletion by ionization in the exhaust region. We show that the results are strongly dependent on the assumptions which are made on the electron mobility. We discuss the influence of this parameter on various discharge characteristics.

I. Introduction

Stationary plasma thrusters (SPTs), also known as Hall thrusters, are advanced electrostatic propulsion devices. [1] In an SPT, a propellant (typically xenon) is ionized by an electrical discharge. The electric field of the discharge subsequently accelerates the produced ions to high exhaust velocities (~ 2×10^4 m/s). Because of the high exhaust velocity SPTs consume (when providing a certain thrust) much less propellant than conventional chemical propulsion devices.

The SPT discharge takes place in an annularly shaped discharge channel. External magnets generate a radial magnetic field in the channel, with a maximum (~ 0.02 T) near the channel exhaust. The discharge voltage (~ 300 V) is applied axially, between an anode at the closed end of the channel and an external hollow cathode, situated beyond the exhaust. The propellant is introduced in the channel via holes in the anode. The gas density (~ 10^{18} – 10^{20} m^{-3}) is so low that the mean free paths of both electrons and ions are much larger than the channel dimensions (~ 10^{-2} m). However, having a small Larmor radius (~ 10^{-3} m), the electrons are confined by the magnetic field: they cycle around the magnetic field lines and at the same time drift in the azimuthal direction (E×B drift, perpendicular to the electric and magnetic fields). Net electron transport in the axial direction (the direction of the electric field) can take place only when collisions occur. The ion Larmor radius is relatively large (~ 1 m) so that the ion motion is nearly unaffected by the magnetic field and collisionless.

To study the SPT discharge operation we have developed a two-dimensional hybrid model. The basic assumptions of the model are similar to those of the 1D model of [2] but electron transport is described more precisely (diffusion is included and the electron energy equation is more accurate). The model is also similar to the model of Fife [3] although the assumptions on the electron conductivity and the numerical techniques are different.

The model is presented in Section II. The most crucial input parameter of the model is the cross field electron mobility. Section III demonstrates the effect of this parameter on the simulation results. The conclusion is given in Section IV.

II. Model

A. Geometry

Only axial and radial dimensions of the thruster geometry and discharge are represented in the model; azimuthal symmetry is assumed. The two-dimensional

[*] Presented as Paper IEPC-01-28 at the 27th International Electric Propulsion Conference, Pasadena, CA, 15-19 October, 2001.

calculation domain, which comprises both the discharge channel and the exterior of the SPT, is shown in figure 1. The discharge is simulated only within a certain region that is confined by physical walls and the magnetic field lines intercepting the electrodes. Note that the magnetic field is curved and not perfectly radial.

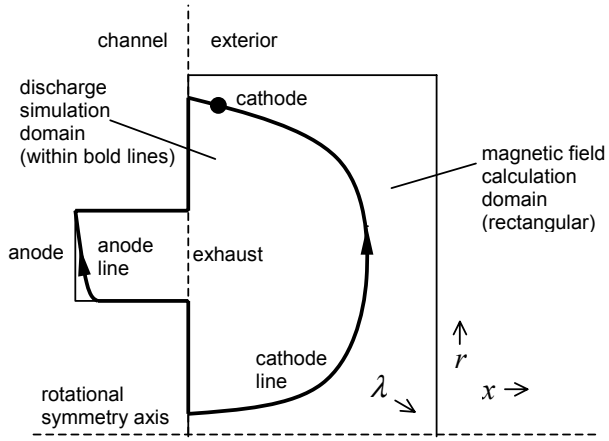

Figure 1 – Schematic picture of the simulation domain

B. Magnetic field

The magnetic field is assumed to be entirely determined by the external magnets and not to be affected by the discharge. This assumption is realistic and makes it possible to calculate the magnetic field *a priori* from

$$\nabla\cdot\mathbf{B}=\nabla\cdot(\nabla\sigma)=0\,, \qquad (1)$$

where **B** is the magnetic field and σ is a magnetic potential. Rather than being calculated directly from the configuration of external magnets, the magnetic field in the discharge channel is obtained from a set of boundary values specified on the domain boundaries. This allows the direct implementation of measured magnetic field data or the deliberate adjustment of the field, which is useful for studying its influence.

As in Fife [3], the magnetic field lines are described by the stream function λ, calculated from

$$\frac{\partial\lambda}{\partial x}=rB_r \text{ and } \frac{\partial\lambda}{\partial r}=-rB_x\,, \qquad (2)$$

where x and r are the axial and radial position coordinates and B_x and B_r are the axial and radial components of the magnetic field. This λ is constant along magnetic field lines ($\mathbf{B}\cdot\nabla\lambda=0$) and usually increases monotonically from anode to cathode. The cross field gradient of any quantity Q can be expressed in terms of λ as

$$\nabla_\perp Q=rB\frac{\partial Q}{\partial\lambda}\,, \qquad (3)$$

which we will use in the following.

C.Neutral gas particles

We consider xenon as a propellant gas. The density of neutral xenon atoms (essential to find the ionization rate and the electrical conductivity of the plasma) is obtained from a Monte Carlo simulation. That is, the individual paths of a large number of neutrals are calculated, where collisions are treated with random numbers. This approach is realistic but takes much computation time and introduces statistical errors. The neutrals are introduced in the simulation at a certain injection region at the anode and are followed until they reach the right boundary of the geometry. Their initial velocity distribution is taken isotropic and Maxwellian with a temperature of 500 K. Only collisions with walls are considered, in which the neutral atoms may be either specularly reflected or diffusely scattered. Neutral loss by ionization is accounted for by gradually decreasing the statistical weight of the simulated neutrals according to the local ionization probability (this introduces less statistical fluctuations than just removing atoms from the simulation).

D. Ions

Only singly charged xenon ions are included in the model. Like the neutrals, the ions are described by a Monte Carlo simulation. The ions are introduced in the simulation at positions that are randomly chosen according to the ionization rate profile. The initial ion velocity distribution is isotropic and Maxwellian at 500 K. The ions are assumed to be accelerated by the electric field only, i.e. to be insensitive to the magnetic field. Ion collisions are not considered. The ions are followed until they reach any of the boundaries of the simulation domain; ions striking the walls are thus assumed to recombine at the surface. Besides the ion density, the ion Monte Carlo simulation yields the ion flux and the ion energy distribution.

E. Electrons

The electrons are described by a fluid model, i.e. the behavior of the electron density, flux, and mean energy is described by the first few moments of the Boltzmann equation (transport equations). This

approach incorporates many assumptions and is not entirely realistic. In view of the high plasma density in SPTs it is assumed that the electron density is everywhere equal to the ion density. With this assumption it becomes impossible to obtain the electric field from Poisson's equation. Instead, knowing the electron density, we use the electron transport equations to calculate the electric field. Note that it is not true that there is no space charge; in reality Poisson's equation is valid.

The electron transport equations are: 1) the coninuity equation

$$\nabla\cdot\Gamma_e = Nnk_i - \frac{\partial n}{\partial t} = \nabla\cdot\Gamma_i \,, \tag{4}$$

2) the momentum equation, which we approximate by the drift diffusion equation

$$\Gamma_e = -\mu\mathbf{E}n - \frac{2}{3}\mu\nabla(\varepsilon n) \,, \tag{5}$$

and 3) the energy equation

$$\frac{\partial(n\varepsilon)}{\partial t} + \frac{5}{3}\nabla\cdot(\mathbf{\Gamma}_e\varepsilon) - \frac{10}{9}\nabla\cdot(\mu n\varepsilon\nabla\varepsilon) = -e\mathbf{E}\cdot\mathbf{\Gamma}_e - Nn\kappa \,. \tag{6}$$

In these equations n is the electron density, $\mathbf{\Gamma}_e$ the electron flux, ε the electron mean energy, N the neutral density, $\mathbf{\Gamma}_i$ the ion flux, $\mathbf{E}$ the electric field, and μ the electron mobility. The ionization coefficient k_i and the effective energy loss coefficient κ are functions of ε. Secondary electron emission from the surface is neglected.

Due to the magnetic field the electron mobility is not a simple scalar: its value is much larger for electron transport along magnetic field lines than for transport across them. As a result the electron density and the electric potential V are (in a good approximation) related by the well-known Boltzmann relation along each magnetic field line:

$$V(x,r) = V^*(\lambda) + \frac{2}{3}\varepsilon(\lambda)\ln n(x,r) \,, \tag{7}$$

where V^* is a function. While V and n vary all over space, V^* and ε depend only on the stream function λ. Note that by using this equation we lose to possibility to calculate the electron flux along field lines from the drift-diffusion equation. From equations (3), (5), and (7), we find for the cross field electron flux

$$\Gamma_{e,\perp} = rB\mu_\perp n\frac{\partial V^*}{\partial\lambda} + \frac{2}{3}rB\mu_\perp n(\ln n - 1)\frac{\partial\varepsilon}{\partial\lambda} \,, \tag{8}$$

where $\mu_\perp$ is the cross field electron mobility.

Let us now define the following (surface) integrals along field lines:

$$c_1 = \int \Gamma_{i,\perp}\,\mathrm{d}l \tag{9}$$

$$c_2 = \int rB\mu_\perp n\,\mathrm{d}l \tag{10}$$

$$c_3 = \int rB\mu_\perp n(\ln n - 1)\,\mathrm{d}l \tag{11}$$

and (volume) integrals between consecutive field lines:

$$c_4 = \iint n\,\mathrm{d}s \tag{12}$$

$$c_5 = \iint Nn\,\mathrm{d}s \tag{13}$$

$$c_6 = \iint -eE_\perp\Gamma_{e,\perp}\,\mathrm{d}s \,. \tag{14}$$

Using these integrals, the continuity and momentum equations (4)-(5) can be replaced by the following one-dimensional equation for current conservation

$$\int\Gamma_{e,\perp}\,\mathrm{d}l = c_2\frac{\partial V^*}{\partial\lambda} + \frac{2}{3}c_3\frac{\partial\varepsilon}{\partial\lambda} = c_1 - \frac{1}{e}I \,, \tag{15}$$

where I is the discharge current. It is assumed that no current escapes to the walls. In a similar way the energy equation can be written as

$$\begin{aligned}\frac{\partial(c_{4,k}\varepsilon_k)}{\partial t} + \frac{5}{3}\left(c_{1,k+1/2} - \frac{1}{e}I\right)\varepsilon_{k+1/2} - \frac{5}{3}\left(c_{1,k-1/2} - \frac{1}{e}I\right)\varepsilon_{k-1/2} \\ - \frac{10}{9}c_{2,k+1/2}\varepsilon_{k+1/2}\left.\frac{\partial\varepsilon}{\partial\lambda}\right|_{k+1/2} + \frac{10}{9}c_{2,k-1/2}\varepsilon_{k-1/2}\left.\frac{\partial\varepsilon}{\partial\lambda}\right|_{k-1/2} \\ = c_{6,k} - c_{5,k}\kappa \,,\end{aligned} \tag{16}$$

where k+1/2 and k-1/2 refer to two field lines, and k to the interval between them. This equation neglects electron transport to the surface.

From the equations (15) and (16) we calculate ε and V^* as a function of λ. Subsequently the spatial profile of the electric potential is found from equation (7). The current I in equation (15) is chosen such, that a specified voltage results between anode and cathode.

III. Electron mobility

A. Model

Probably the most crucial input parameter of the model is the cross field electron mobility $\mu_\perp$: this parameter is hardly known but has a strong influence the simulation results.

The classical expression for $\mu_\perp$ is given by

$$\mu_\perp = \frac{e\nu_m/m_e}{\nu_m^2 + (eB/m_e)^2} \approx \frac{m_e\nu_m}{eB^2} \,, \tag{17}$$

where e is the elementary charge, m_e the electron mass, and ν_m the momentum transfer frequency. It is clear however the classical mobility is too low to be realistic for the electron transport in SPTs, especially near and beyond the exhaust where the gas density is very low.

Apparently there are additional mechanisms of electron transport. One mechanism likely to play a role is momentum transfer due to collisions with the channel walls. The frequency of these collisions depends on the radial electron velocity and the plasma sheath voltage, and is very difficult to calculate accurately; estimates yield 10^6 – 10^7 s^{-1}. Inside the channel we include (in a crude approximation) a constant contribution of wall collisions in the ν_m in equation (17)

$$\nu_m = \nu_{m,\mathrm{vol}} + \alpha \times 10^7 , \qquad (18)$$

where the two terms represent volume collisions and walls collisions, and α is a fit parameter. This approach has been succesfully applied previously. [2]

Cross field electron transport may also be enhanced by anomalous Bohm mobility, resulting from small fluctuations in the magnetic field. [3] The Bohm mobility is proportional to $1/B$; an empirical proportionality constant of 1/16 has been found for some magnetized plasmas. Although Bohm mobility has not directly been measured in SPTs, it might exist especially where the magnetic field strength increases in the direction of the electron transport, i.e. at the exterior of the SPT. Outside the channel we use therefore

$$\mu_\perp = \mu_{\perp,\mathrm{clas}} + \frac{K}{16B} , \qquad (19)$$

where the two terms represent the classical cross field mobility of equation (17) and Bohm mobility, and K is a fit parameter.

Our electron mobility thus contains two fit parameters: α inside and K outside the channel. Below we show how by changing these parameters we can completely change the characterics of the simulated discharge.

B. Parametric study

Let us first consider the case that α=0.1 and K=1; this yields simulation results that are not entirely unrealistic. Figure 2 shows the calculated potential, plasma density, and ionization rate. The electric field is strongest near the exhaust, where the cross field electron mobility is smallest due to the large magnetic field and the low neutral density. In this so-called acceleration region the ions obtain their high exhaust velocity, and the electron mean energy reaches several tens of eVs, resulting in ionization of the propellant gas. With respect to the acceleration region the ionization maximum is shifted inward, where the neutral density is higher. High neutral density even causes an additional local ionization maximum at the gas inlet. The plasma density is highest in the center of the channel and decreases in the accerelation region due to the increasing ion velocity.

As is to be expected, the position and size of the acceleration region are directly determined by the choice for α and K. When we increase α and decrease K, the acceleration zone shifts to the exterior of the channel. The maxima in plasma density and ionization rate follow. This is illustrated by figure 3. Note that the electric field is discontinuous at the exhaust as a result of the discontinuity in the assumed electron mobility. When assuming a continous mobility ($\alpha/K \approx 0.07$), the acceleration region turns out to always be entirely located outside the channel.

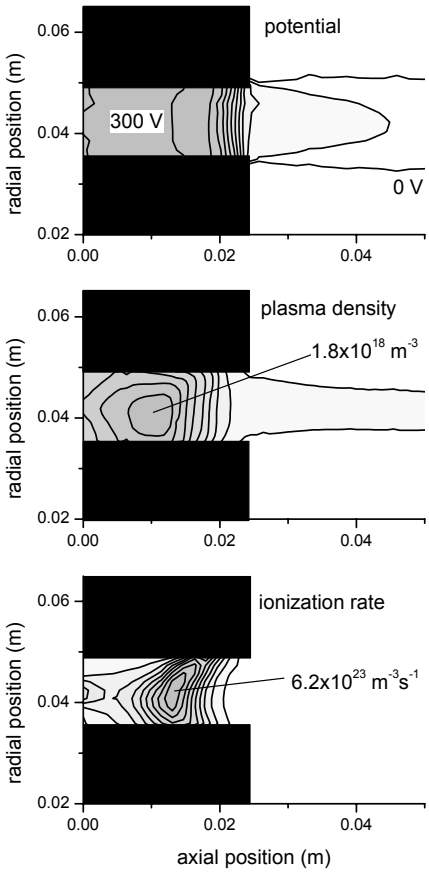

Figure 2 – Electric potential, plasma density, and ionization rate in a typical SPT discharge simulation. The horizontal axis gives the axial distance to the anode. The increment of the contours is 1/10 times the maximum value indicated in each plot.

In figure 3 we varied both α and K at the same time, in order to obtain similar discharges: In each of the cases the discharge is stable, has a current of about 2.5 A and an ionization maximum located near the acceleration region. When decreasing α keeping K constant, the simulated discharge starts to show high frequency oscillations (80–150 kHz). See figure 4 for illustration: If K=1, the current oscillates for α=0.03 and is stable for α=0.1. Note the statistical noise due to the Monte Carlo method. The shown high frequency current oscillations are related to local plasma density maxima moving outward with the ion exhaust velocity. If both α and K are small (α=0.003, K=0.1 in figure 4) additional low frequency oscillications are present (10–20 kHz). These low frequency oscillations have been reported previously [2] and are related to the depletetion of neutrals.

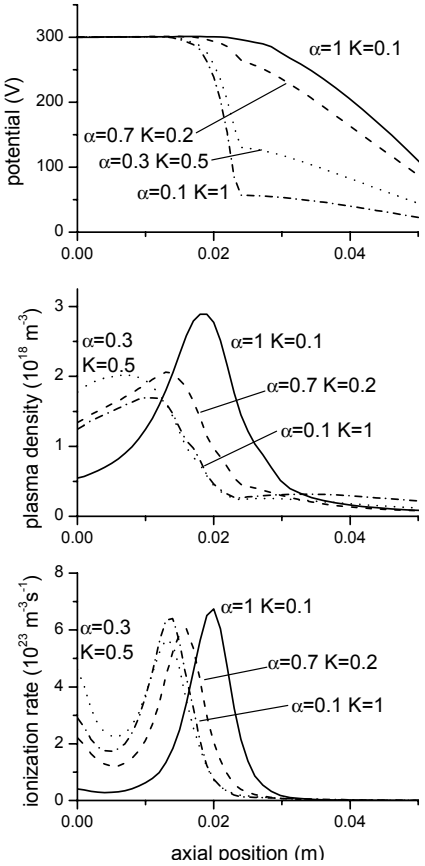

Figure 3 – Axial profiles in the center of the channel of the electric potential, plasma density, and ionization rate, for various combinations of α and K.

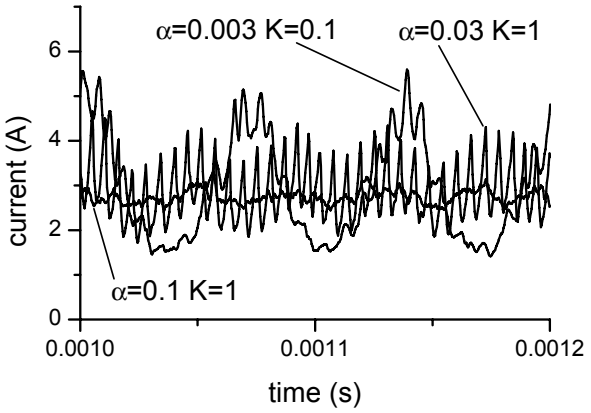

Figure 4 – Discharge current as a function of time for various combinations of α and K.

Finally, we remark that for high α and K the discharge shifts to a different regime, characterized by a low current (<1 A) and a strong ionization maximum at the gas inlet; this seems hardly realistic.

IV. Conclusion

We have developed a two-dimensional hybrid model of a SPT. The model provides the space and time variations of the plasma density, neutral atom density, electric potential, and ionization rate inside and outside the SPT channel. The model can simulate steady sate operations of a SPT in a few tens of CPU minutes on a 1 GHz Pentium. The numerical code is robust and different magnetic field distributions can be easily tested.

The results of the two-dimensional model reproduce the low frequency oscillations described in previous works. The electron conductivity is still not well understood in the SPT and the role of electron scattering with the walls or field fluctuations is difficult to quantify precisely. We therefore chose to characterize the effect of wall scattering or Bohm conductivity by two parameters. The results show that the current oscillations and electric potential distribution depend heavily on these parameters. Systematic comparisons between model predictions and experimental measurements will help choosing the parameters characterizing the electron mobility.

Acknowledgements

The 2D SPT model has been developed in the framework of the Groupement De Recherche CNRS/CNES/SNECMA/ONERA 2232 "Propulsion Plasma pour Systèmes Spatiaux".
G.H. would like to acknowledge support from the European Office of Aerospace Research and Development, Air Force Office of Scientific Reseach, Air Force Research Laboratory, under contract No. F61775-01-WE015.

References

[1] A. Cadiou, M. Lyszyk, and M. Dudeck, 26th International Electric Propulsion Conference, paper IEPC-99-007 (Kitakyushu, Japan, 1999).

[2] J. P. Boeuf and L. Garrigues, J. Appl. Phys. **84**, 3541 (1998).

[3] M. Fife, Thesis, MIT (1998)

[4] V. V. Zhurin, H. R. Kaufmann, and R. S. Robinson, Plasma Sources Sci. Techn. **8**, R1 (1999).